

# Optical Recording from Populations of Neurons in Brain Slices

SAURABH R. SINHA and PETER SAGGAU

## ■ Introduction

Optical recording involves the use of molecular indicators whose optical properties (absorbance or fluorescence) change with parameters of cellular activity. Available indicators include those sensitive to membrane potential ( $V_m$ ), to calcium concentration and to concentrations of other ions ( $H^+$ ,  $Na^+$ ,  $K^+$ ,  $Mg^{2+}$ ,  $Zn^{2+}$  and  $Cl^-$ ). Optical recording provides several advantages over conventional approaches. In the case of electrical activity, even heroic efforts involving large arrays of microelectrodes (e.g., Breckenridge et al. 1995) cannot give the spatial resolution that can be obtained relatively easily with optical approaches with significantly less damage to the preparation. Optical techniques also allow for recording from sites inaccessible to conventional approaches. In the case of ionic concentrations, they also provide higher temporal resolution than conventional methods such as ion-sensitive electrodes. Application of optical recording techniques to single neurons in culture is discussed in Chapter 4 (Bullen and Saggau). In the present chapter we describe techniques for optically recording from populations of neurons in mammalian brain slices. These techniques are illustrated with examples from our laboratory of recording membrane potential and intracellular calcium concentration ( $[Ca^{2+}]_i$ ) from rodent hippocampal slices. First, we briefly discuss some of the basic issues involved including optical indicators, loading techniques, optical filters and photodetectors. Intrinsic optical properties of brain tissue are also discussed but only in so far as they affect measurement of signals from optical indicators. Chapter 34 (Grinvald et al.) deals with how intrinsic optical properties can be used to record activity in intact brain structures.

## Optical Indicators

In this section we briefly discuss the characteristics of some commonly used optical indicators with emphasis on voltage-sensitive and calcium-sensitive dyes, the two types of optical indicators used in the protocols described in this chapter. Additional details on these indicators are given in chapter 4 (Bullen and Saggau) of this book; furthermore, detailed information on most commercially available optical indicators can be found in the Molecular Probes catalog (Haugland 1996).

Voltage-sensitive dyes (VSDs) are molecules whose optical properties reflect either the membrane potential or changes in  $V_m$  (for review see Cohen and Leshner 1986; Ebner and Chen 1995). VSDs can be subdivided into two classes based on the speed of their response. "Slow" VSDs are membrane permeable and distribute themselves across the

Voltage-sensitive Dyes

**Table 1.** Dyes and Optical Filters/Dichroic Beam Splitters

Indicator	Type	$K_d$ (nM)	$\lambda_{ex}$ (nm)	$\lambda_{em}$ (nm)	EX Filter (nm)	DB (nm)	EM Filter (nm)
RH-155	Abs	--	638	--	650/40	--	--
RH-414	Fluor	--	531	714	535/45	605	610LP
Calcium Orange-AM	Fluor	328	549	575	535/45	565	570LP
Fura-2-AM	Fluor	224	335,362	512	360,380/10	450	510/40
Fura-2-AM	Fluor	50,000	330,370	511	360,380/10	450	510/40

cell membrane according to the Nernst equation. These indicators can be useful for measuring slow changes in  $V_m$  but are generally not of use for measuring fast changes such as those encountered during neuronal activity. "Fast" VSDs are amphipathic molecules that insert into the cell membrane and exhibit potential-dependent changes in either absorbance ( $A$ ) or fluorescence ( $F$ ). Their response times are in the range of microseconds; the response of VSDs to change in membrane potential is linear in the physiological range (Ross et al. 1977), i.e., the change in absorbance ( $\Delta A$ ) or fluorescence ( $\Delta F$ ) is proportional to the change in membrane potential ( $\Delta V_m$ ). Several non-fluorescent (e.g., RH-155 and RH-492) and fluorescent (e.g., RH-414 and RH-795) fast VSDs have been used in brain slices. Absorbance measurements have the chief advantage that for a given intensity of incident light, the intensity of light reaching the detector will be larger than it would be for a fluorescence measurement; also, the setup required for an absorbance measurement is marginally simpler than one for fluorescence (see Fig. 1). On the other hand, fluorescence measurements generally provide slightly larger fractional changes in the signals compared to absorbance measurements,  $\Delta F/F \sim 10^{-3}$  versus  $\Delta A/A \sim 10^{-4}$ . Another fact about VSDs to keep in mind is the same VSD may behave very differently in different preparations; this is most likely related to differences in the composition of the plasma membranes. Thus, it is usually necessary to screen several VSDs whenever using them in a new preparation. Some of the VSDs commonly used in our lab are listed in Table 1 along with the characteristics of the optical filters used with them.

Due to their amphipathic nature, VSDs are very difficult to load into individual cells. Significant success with intracellular loading of VSDs has been reported only in invertebrate preparations with large cells that can be kept viable for long periods of time after injection (>12h). This is necessary to allow for pressure injection of large quantities of dye and for subsequent diffusion of dye into the processes (Zecevic 1996). Thus, although some initial success has recently been reported with loading VSDs into individual neurons in brain slices (Antic et al. 1997), VSDs are generally bath-applied for optical recording from both single neurons in culture and from populations of neurons in brain slices. There are some initial reports of selective loading of VSDs into certain subpopulations of neurons by retrograde transfer of dye by cut axons in some preparations (Wenner et al. 1996).

### Calcium-sensitive Dyes

Calcium-sensitive dyes (CaSDs) are calcium chelators whose optical properties change upon binding  $Ca^{2+}$ . Absorbance measurements are rarely used with CaSDs today. Most modern CaSDs were derived from the calcium chelator BAPTA by conjugation with various fluorophores (Tsien 1980; Grynkiewicz et al. 1985; Minta et al. 1989). These highly fluorescent compounds bind only one  $Ca^{2+}$ , with high selectivity over  $Mg^{2+}$  in the physiological range, and with relative insensitivity to  $H^+$ . Upon binding  $Ca^{2+}$ , either the efficiency with which they absorb photons (extinction coefficient,  $\epsilon$ ) or the efficiency with

which they convert an absorbed photon to an emitted one (quantum efficiency) is altered. For several of these indicators, there is an actual wavelength shift in their absorption (Fura-2, Fura-2/AM) or emission (Indo-1) spectra; this allows for ratiometric calibration of the signals. However, this is generally not useful when recording from groups of neurons, as the value will actually be an average of the concentrations in several cells and is relatively meaningless unless it is assumed that all the loaded cells are in the same state of activity.

Unlike VSDs which respond linearly to changes in membrane potential, physiological changes in  $[Ca^{2+}]_i$  can be such that the response of the CaSD may not be linear.  $Ca^{2+}$  binding to CaSD is a first order chemical reaction with a dissociation constant,  $K_d$ , an on-rate constant,  $k_{on}$ , and an off-rate constant,  $k_{off}$ . For any given CaSD, the change in fluorescence is approximately linear to the change in  $[Ca^{2+}]_i$  over the range  $0.1K_d$  to  $10K_d$ . A nonlinear response will be observed both below and above this range. Thus, the range of expected  $[Ca^{2+}]_i$  is an important consideration in selecting a CaSD for a particular application. For example, if one is interested in detecting changes in calcium concentrations near the resting level ( $\sim 100$  nM in most neurons), a CaSD with a  $K_d$  in the range of hundreds of nanomolar is most appropriate, e.g., Fura-2 or Calcium Orange (see Table 1). However, if one is instead interested in relative changes in the peak levels of calcium concentration in synaptic terminals following a single action potential or a train, an indicator such as Fura-2/AM with a  $K_d$  of tens of micromolar is more appropriate. Also because the CaSD signal depends on actual binding and unbinding of  $Ca^{2+}$  to the calcium indicator, the time course of the signal depends on the kinetics of this reaction as well as the actual change in  $[Ca^{2+}]_i$ . The time constant of the rise in the CaSD signal ( $\tau_{on}$ ) for a step rise in  $[Ca^{2+}]_i$  is:

$$\tau_{on} = \frac{1}{k_{on} \cdot ([Ca^{2+}] + [CaSD]) + k_{off}}$$

For a step decline, the time constant of the fall in the CaSD signal ( $\tau_{off}$ ) is:

$$\tau_{off} = \frac{1}{k_{off}}$$

Most of the modern indicators have a similar  $k_{on}$ , being close to diffusion-limited; therefore, the kinetics of their responses are determined by their  $K_d (= k_{off}/k_{on})$ . The higher the  $K_d$ , the faster the response and the more accurately the time course of the CaSD signal reflects the time course of  $[Ca^{2+}]_i$ . Indicators with a high  $K_d$  also have the advantage that they are less likely to be saturated and are less likely to significantly contribute to the calcium buffering properties of the neuron. For a more detailed discussion of these issues, see Sinha et al. (1997). The  $K_d$  values of the indicators we use routinely are given in Table 1.

In order to record  $[Ca^{2+}]_i$ , these indicators must be loaded into the cells of interest. If the only available means for loading these indicators were to inject them using microelectrodes, recording from any significant number of cells would not be possible. Loading of CaSDs was greatly simplified by the advent of acetoxymethyl (AM) esters of these indicators (Tsien 1981): these esters are membrane permeable but become trapped inside cells when cleaved by intracellular esterases. Thus, preparations can be loaded by simply bathing slices in the AM ester of the CaSD. This type of loading is very useful when non-selective loading of a large number of cells is desired instead of selective loading of a single cell. Local application of AM esters to selected anatomical structures such as axon tracts in some preparations allows for the selective loading of subcellular structures such as presynaptic terminals (Regehr and Tank 1991; Wu and Saggau 1994) or dendrites (Wu and Saggau 1994). The specific CaSDs that we regularly use in our laboratory are listed in Table 1.

## Other Ion-sensitive Dyes

As mentioned previously, optical indicators that are sensitive to ions other than  $\text{Ca}^{2+}$  are commercially available (e.g.,  $\text{H}^+$ ,  $\text{Na}^+$ ,  $\text{K}^+$ ), many in the AM ester form which allows for loading into populations of neurons. However, we have not used any of these indicators in our laboratory for recording transients in brain slices, nor are we aware of other investigators who have done so. The main issues involved in using these indicators to record from populations of neurons should be the same as those for CaSDs. Several of these indicators have been used in cell cultures and in individually loaded neurons in brain slices. pH-indicators are available with various spectral characteristics and sensitivities ( $\text{pK}_a$ ); examples include BCECF, SNAFL and SNARE.  $\text{Na}^+$ -sensitive dyes that are amenable to loading into populations of neurons include SBFI and Sodium Green; PBFI is a  $\text{K}^+$ -sensitive dye that is also available as an AM ester. A general problem with currently available potassium and sodium indicators is relatively poor selectivity between the two ions. For more details on these and other ion-sensitive indicators (e.g.,  $\text{Cl}^-$  or  $\text{Zn}^{2+}$ ), the reader is referred to the Molecular Probes catalog (Haugland 1996). This is also an excellent source for information about new optical indicators, which are constantly being developed.

## Microscopes

Several types of microscopes can be used in optical recording applications using brain slices including conventional microscopes, scanning microscopes, confocal microscopes and various combinations of the above (for a more detailed discussion of the various types of microscopes, see chapter 4, Bullen and Saggau). In this chapter, our discussion will be limited to conventional microscopes. A schematic of a basic setup for absorbance measurements is shown in Fig. 1A. It should be noted that only water-immersion objectives with their small working distances (e.g.,  $\sim 1.7$  mm for 40 $\times$ , 0.9NA, Zeiss) can be used for absorbance measurements. Air objectives cannot be employed with submerged brain slices, as ripples at the air-liquid interface will cause changes in the amount of light reaching the detectors. These changes can be much larger than the actual optical indicator signal (recall that fractional changes in the absorbance of an optical indicator are typically well below 0.1%). The main problem with small working distance is that micropipette access is severely limited. Even using an inverted microscope would not avoid this problem, since in the case of an absorbance measurement, a water immersion condenser would be necessary.

For fluorescence measurements, an inverted microscope is preferable for several reasons: (1) the top of the recording chamber is not hindered by the presence of an objective lens, allowing easy access for micropipettes; and (2) both air and oil immersion objectives can be used. Fig. 1B is a schematic of the basic inverted epifluorescence microscope setup that we use in our laboratory. However, upright microscopes have their own advantages; for example, with an upright microscope, the side of the preparation to which one has micropipette access is also the side from which most of the optical signals are emerging. This is an important consideration when recording from single cells in a brain slice. Fig. 1C shows a schematic of an upright epifluorescence microscope. As discussed above, the only option is a water immersion objective for such a setup.

The performance characteristics of a conventional microscope are largely determined by its objective lens. The two main characteristics of an objective are its magnification (*mag*) and its numerical aperture (*NA*). The magnification determines the size of the area seen by the objective; in conjunction with the number of individual elements in the photodetector, this determines the spatial resolution of the optical signal. The *NA* describes the light gathering capability of the objective: the higher the *NA*, the larger the fraction of light emanating from the preparation that is collected by the objective (for

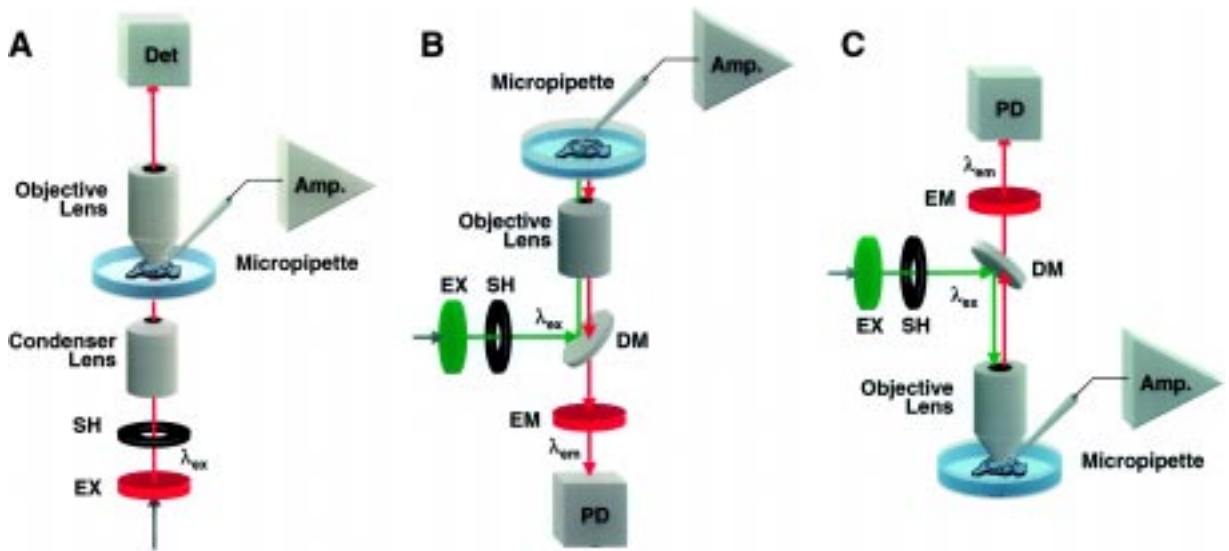


Fig. 1. Schematics of typical optical recording setup. **A.** Microscope for absorbance measurement. Light is limited by an excitation filter (EX) to the appropriate wavelength ( $\lambda_{ex}$ ), an electromechanical shutter (SH) to control the time of illumination and is directed onto the preparation via a condenser lens. Transmitted light is collected by the objective lens (water-immersion) and quantified by a photodetector (Det). **B.** Inverted microscope for epifluorescence measurement. Excitation light ( $\lambda_{ex}$ ) is directed onto the preparation by a dichroic beamsplitter (DB) and the objective lens (air or oil-immersion). Fluorescence emitted from the preparation ( $\lambda_{em}$ ) is collected by the same lens, passes the DB, is filtered by the emission filter (EM) and quantified by DET. **C.** Upright microscope for epifluorescence measurement. Setup is analogous to that in B, except that it is now in an upright configuration, utilizing a water immersion lens.

an oil immersion objective, the upper limit for  $NA$  is 1.4). The magnification also affects how much light is collected by the objective because it determines the size of the area from which the objective collects light and, thus, the number of fluorescent molecules. For an epifluorescence microscope, the image intensity is proportional to:

$$\frac{NA^4}{mag^2}$$

This relationship can be used to determine the characteristics needed for an objective, the most common scenario being that one has an objective lens of a given  $mag$  and  $NA$  that collects sufficient light for a given application and now a different  $mag$  is desired. The above equation can be used to determine the  $NA$  the new lens should have to collect the same amount of light. The objective lenses that we commonly use are listed in Table 2.

Table 2. Objective Lenses

Objective	NA	Type	WD (mm)	$NA^4/mag^2 \times 10^{-4}$
5x	0.25	Air	5	1.56
10x	0.5	Air	0.88	6.25
25x	0.8	Oil/water	0.13	6.55
40x	0.75	Water	1.7	1.98
40x	0.9	Oil/water	0.13	4.10
50x	0.9	Oil	0.3	2.62
63x	0.9	Water	1.7	1.65

Other integral parts of an optical imaging setup include the light source, shutter, optical filters and photodetectors. Filters and detectors are discussed below. The two types of light sources we commonly use are a tungsten halogen lamp and a xenon burner (see chapter 4, Bullen and Saggau for a more detailed discussion of light sources). The chief advantage of the tungsten lamp is that it can be operated with a battery-powered source providing very high amplitude stability (RMS noise  $\sim 10^{-5}$ – $10^{-4}$ ). The reason for using the noisier xenon burner (RMS noise  $\sim 10^{-3}$ – $10^{-4}$ ) is that it is  $\sim 5\times$  brighter than the tungsten lamp; the relative brightness of the xenon burner is even higher at short wavelengths, i.e., near the ultraviolet range. Due to noise considerations, mercury burners are usually not advisable. An electromechanical shutter is necessary in order to limit the periods of light exposure to only the actual recording periods.

### Optical Filters

Optical filters are an integral part of any optical recording setup. A brief description of the more commonly used types of filters is given here; the exact specifications of the filters used with various indicators are given in Table 1. A bandpass filter is characterized by its center wavelength (the wavelength at which it has maximal transmission) and its full-width at half-maximal transmission (the range of wavelengths over which the filter transmits  $>50\%$  of its maximal transmission). These numbers are usually expressed as center/FWHM (e.g., 535/25 nm). A longpass filter transmits all visible wavelengths above its characteristic wavelength (the wavelength at which it transmits 50% of its maximum). A dichroic beamsplitter is a hybrid of an optical filter and mirror which reflects all light below its characteristic wavelength and transmits all light above it.

Fig. 2 shows the relationship between the filters and the excitation and emission spectra of an optical indicator. In a typical optical recording setup equipped for epifluorescence (Fig. 1B,C), the excitation filter has bandpass properties and the emission filter is either bandpass or longpass. The dichroic beamsplitter has a characteristic wavelength in between the emission and excitation filter so that it can separate the excitation and emission light.

### Photodetectors

Several types of photodetectors are available today, differing in sensitivity, spatio-temporal resolution and intensity resolution. We will first discuss characteristics of photodetectors in general and then specifically describe the types of optical detectors we use in our laboratory. Additional information on this topic is given in Chapter 4 of this book (Bullen and Saggau).

#### General Considerations About Photodetectors

The sensitivity of a photodetector is proportional to the number of electrons that are generated for each photon that is absorbed by the detector (quantum efficiency, QE). Silicon photodiodes have the highest quantum efficiencies with  $QE > 0.8$  and, therefore, are the detectors of choice with respect to sensitivity.

Spatial resolutions of available photodetectors cover a large range, from single photodiodes with no spatial resolution, to photodiode matrices (PDMs) with relatively low spatial resolution, to charge-coupled device (CCD) cameras with high spatial resolution. While high QE values also apply to PDMs, most CCD cameras have significantly lower values ( $QE \sim 0.5$ ) due to their complex layout. There are two main tradeoffs that come with increasing spatial resolution. First, the higher the number of individual ele-

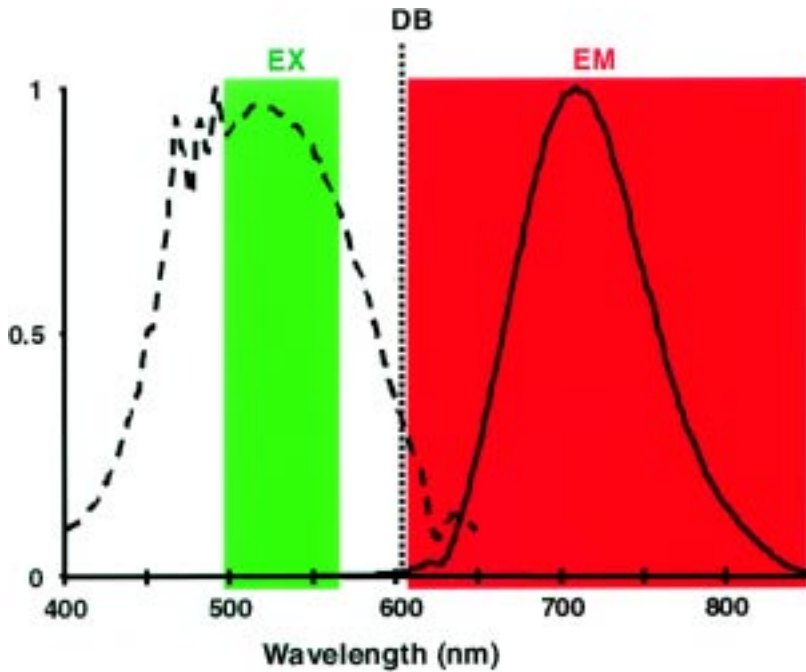


Fig. 2. Selection of optical filters and dichroic mirror. Excitation (*dashed line*) and emission (*solid line*) spectra of fluorescent indicator (specifically the VSD RH-414) are shown along with typical characteristics of the excitation filter (EX), dichroic beamsplitter (DB) and emission filter (EM).

ments in the detector, the lower the amount of light that reaches any given element. Second, the larger the number of elements, the more data that must be gathered, thus reducing the speed of data collection. This is a more significant problem for CCD cameras because most are serial readout devices and data from all the elements must pass through a single amplifier.

The temporal resolution of a photodetector refers to the speed with which a complete frame of data can be collected; the intensity resolution refers to the smallest fractional change in signal (typically voltage, thus  $\Delta V/V$ ) that can be recorded. Both of these resolutions have to be matched by the characteristics of the analog-to-digital (A/D) converter used: the conversion rate for temporal resolution and the number of bits for the intensity resolution. For CCD cameras, the A/D converter is typically an integral part of the device, while this is not the case for single photodiodes and PDMs. With respect to conversion rate, the minimum sampling frequency necessary to record a signal of bandwidth  $\Delta f$  is

$$f_{\text{sample}} = 2 \cdot \Delta f \cdot N,$$

where  $N$  is the number of elements in the detector. For an  $m$ -bit A/D converter, the intensity resolution is:

$$\frac{\Delta V}{V} = 2^{-m}.$$

Thus, intensity resolution for a 16-bit converter is  $\sim 1.5 \times 10^{-5}$ ; for a 12-bit converter, it is  $\sim 2.5 \times 10^{-4}$ . For a given price range, there is typically a tradeoff between the number of bits and the conversion rate an A/D converter provides. This requires one to critically

balance the need for intensity resolution versus temporal and spatial resolution as the spatial resolution affects the conversion rate necessary to obtain a desired frame rate.

### Specific Photodetectors

The simplest and least expensive detector is the single photodiode, which provides very high temporal resolution and sensitivity but no spatial resolution. A single photodiode detector with the appropriate amplifiers can be built for less than \$50.00 in components; furthermore, such detectors are commercially available. A schematic of the amplifier that we use for single photodiodes is shown in Fig. 3. The response time constant of this photodiode is mainly determined by the capacitance of the photodiode itself and the feedback resistance of the first stage ( $R_f$ ); for typical values of components shown in Fig. 3, response time constants range from  $<100\mu\text{sec}$  to 1 msec. For single photodiodes ( $N=1$ ), A/D converters with sufficiently high intensity resolution and high digitization rates are easily available (e.g., 16-bit and 10kHz). A single photodiode thus makes an ideal detector for situations where spatial resolution is not an issue; our laboratory uses single photodiodes routinely to record CaSD signals from selectively loaded pre- or postsynaptic structures in hippocampal slices. Also, because of its low cost, flexibility and ease of implementation, it is an ideal detector for pilot studies involving new preparations, dyes, loading techniques or equipment.

The two main options that are currently available for recording spatially resolved signals are photodiode matrices (PDMs) and cooled CCD cameras. The latter have the advantage of high spatial resolution (several hundred pixels in each dimension). They also have the capability for temporal integration on the detector chip and the flexibility to vary their spatial resolution by integration of pixels (binning). This integration feature makes them especially useful in low light applications. The main disadvantage of CCD

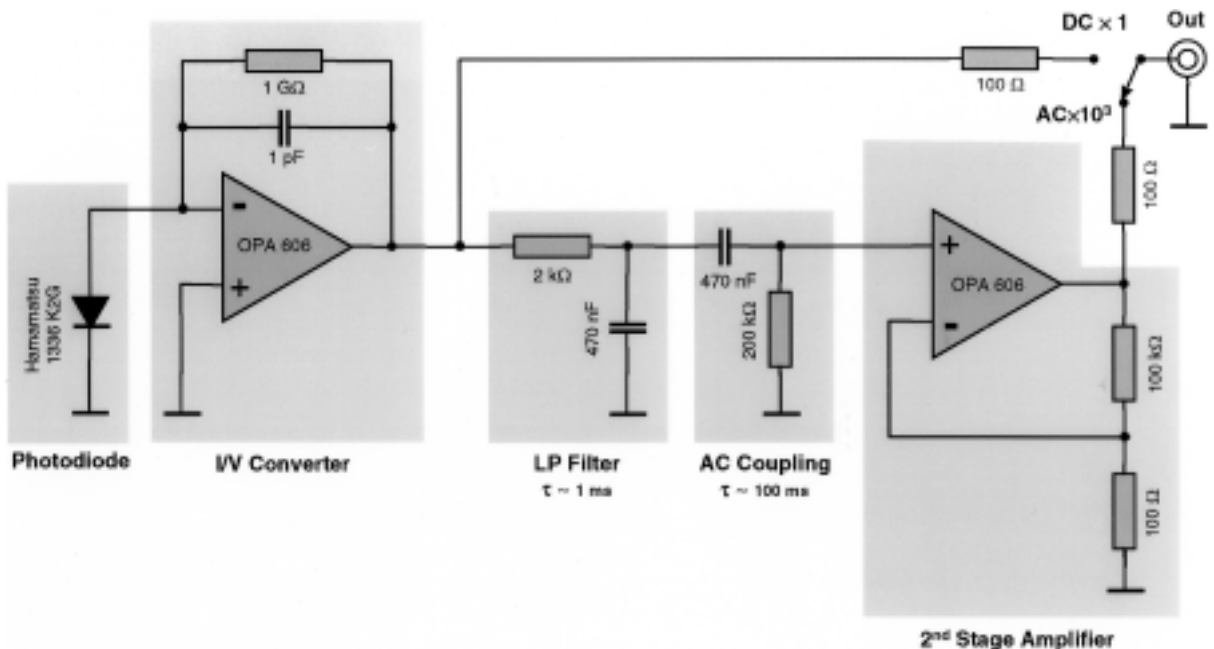


**Fig. 3.** Amplifier for single photodiode. The amplifier consists of an I-V converter, the output of which is directly available (DC  $\times 1$ ) and also forms the input to the second stage of the amplifier. The trans-impedance amplification of the first stage is due to the feedback resistor  $R_f$ ; its time constant is  $R_f C_f$ . The second stage is preceded by a low-pass filter (LP filter) and provides an additional AC-amplification (AC  $\times 1000$ ).

Table 3. Photodetectors

Photodetector	Sensitivity	Spatial Res.	Temporal Res.	Intensity Res.	Ease of Use	Cost
Photodiode	+++	+	++++	++++	+++	+
PDM	+++	+++	+++	+++	+	+++
CCD camera	++	++++	+ / ++	+	++	+++

cameras relates to their usually low temporal resolution and sensitivity. Due to their serial readout scheme, their temporal resolution only approaches a few hundred frames/sec, even with substantial spatial integration (Lasser-Ross et al. 1991). In practice, their temporal resolution is even lower due to temporal integration, which is often necessitated by their low sensitivity to light. However, back-thinned CCD cameras with QEs approaching that of photodiodes have recently become commercially available. Also, newly developed CCD cameras with multiple readout amplifiers may overcome the speed problem. Another limitation is that most currently available CCDs only provide 12-bit intensity resolution; therefore, they can at best measure a fractional change of  $\sim 2.5 \times 10^{-4}$ , which is not sufficient to record the fractional changes observed with VSD signals but is sufficient to record some CaSD signals. For example, CCD cameras have been used to record transients in individual mossy fiber terminals in hippocampal slices in which mossy fibers were selectively loaded with CaSD (Regehr and Tank 1991; Wu and Saggau, unpublished observation).

The detector that we use for most applications requiring spatial resolution is the photodiode matrix. PDMs allow for a reasonable compromise between the high spatial resolution of CCDs and high intensity and temporal resolution of single photodiodes; furthermore, their QE is similar to that of single photodiodes. PDMs are available in various configurations from  $2 \times 2$  to  $128 \times 128$  (Centronic, Hamamatsu, Fuji). Each element of the PDM requires its own amplifier analogous to the single photodiode amplifier shown in Fig. 3. For the  $10 \times 10$  PDM that we use (MD-100, Centronic), this means that 100 individual amplifiers are necessary. In such a case, physical placement of these amplifiers near the PDM becomes a challenge. We have overcome this problem by building an amplifier consisting of stacks of circuit boards on which the various stages of 100 individual amplifiers are located in parallel. The building of such an amplifier is likely to be outside the reach of many users; PDMs with amplifiers are now commercially available from several sources (e.g., Hamamatsu, OptImaging).

In addition to the physical requirements placed on the amplifier for the PDM, additional requirements on the design are placed by the need to digitize a large number of channels at a high sampling rate with sufficient intensity resolution. A/D converters with sufficiently high sampling frequencies to record from large arrays and with high intensity resolution are available; however, they are very expensive. Instead, we use a relatively straightforward procedure to increase the virtual intensity resolution of a fast (400 kHz sampling frequency) 12-bit A/D converter. This procedure relies on the use of AC coupling and subsequent amplification to measure the optical signal which consists of a large static component (static fluorescence,  $F$ ) and a much smaller component that changes with the parameter being measured ( $\Delta F$ ). The static fluorescence from the brain slice is first measured with the amplifier in DC coupling mode with an amplification of 1; the fluorescence transient during the activity to be recorded is measured in AC coupling mode with a gain of  $10^3$ . This additional gain of  $10^3$  effectively extends a 12-bit into a 22-bit A/D converter ( $10^3 \approx 2^{10}$ ). A schematic of the amplifier we use for our PDM

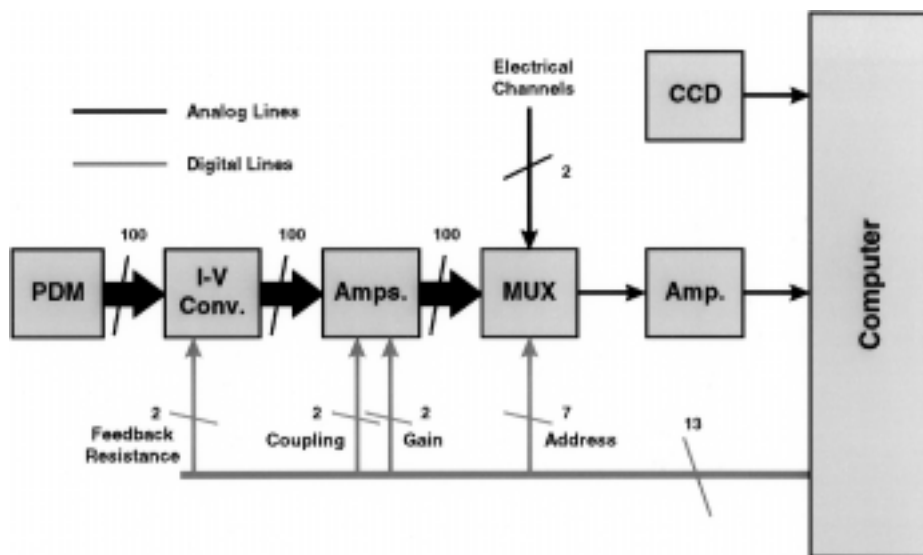


Fig. 4. Amplifier for PDM. The amplifier consists of 100 two-stage amplifiers similar to the single photodiode amplifier shown in Fig. 3. The outputs of these amplifiers are multiplexed (MUX) together with two additional external channels, one of which is used for the microelectrode signal. A single channel amplifier is located after the MUX for additional gain; its output is digitized by the computer. The signal from a CCD camera, which is used to obtain a background image of the recording area, is also fed into the computer. Digital lines from the computer control various amplifier characteristics such as feedback resistance of the I-V converter, AC- versus DC-coupling, gain of second stage, and the MUX address.

is illustrated in Fig. 4. A disadvantage of using AC coupling is the need to increase the duration of light exposure for the preparation. When an AC-coupled amplifier is first exposed to light (opening of shutter), a voltage transient is observed, which settles back to baseline with its characteristic AC time constant (100 msec for our design). Therefore, after opening the shutter, one needs to wait  $\sim 5$ – $10$  time constants ( $> 500$  msec) before starting to record. With DC coupling, this delay only needs to be long enough for mechanical artifacts from the shutter opening to decay before starting to record (typically  $< 50$  msec).

## Tissue Properties

Autofluorescence refers to the fluorescence intrinsic to the tissue. It is mainly due to intracellular aromatic molecules such as FAD and tryptophan. While there have not been any systematic studies of autofluorescence, several basic principles are well established.

- Autofluorescence depends on the wavelength of the excitation light: it is highest for low excitation wavelengths (UV to blue); for higher excitation wavelengths such as green light (500–540nm), it is almost negligible. Thus, autofluorescence is a significant issue when using indicators excited at short wavelengths such as Fura-2 or Furaptra, but is not a factor when using RH-414 or Calcium Orange, which are excited by green light.
- The level of autofluorescence is highly variable; it varies depending on the type of tissue (even within different regions of the same brain slice), the animal species being used and the age of the animal.

Thus, regardless of the indicator being used, it is important to measure the level of autofluorescence and to correct for it. Ideally, one would like to measure the autofluorescence at the exact location where one is recording; however, this is usually not practical. A reasonable compromise is to measure the autofluorescence in the corresponding region in a separate brain slice from the same animal or, in the case of selective loading of pre- or postsynaptic structures, to measure the autofluorescence in a corresponding region which has not been stained.

Another tissue property to keep in mind when recording optically from brain slices is that most tissues scatter light extensively. The main effect of light scattering on optical recording from brain slices is that it places a limitation on the spatial resolution possible regardless of the level of magnification or the number of elements in the detector. As with autofluorescence, the amount of scattering is highly variable; unfortunately, unlike autofluorescence, it is difficult to correct for light scattering. Scattering increases with the thickness of the tissue and varies inversely with the wavelength of light, i.e., higher scattering for shorter wavelengths. Therefore, multi-photon excitation of fluorescent indicators in the infrared has been demonstrated to significantly decrease this effect, allowing for optical recording from non-superficial structures in light scattering preparations (for review see Denk and Svoboda 1997).

## ■ Outline

As must be apparent from the above discussion, many issues need to be considered before attempting to record optical signals from a brain slice preparation. Each application must be customized with respect to the indicator used, loading technique, microscope, objective, optical filters and photodetectors. Fig.5 shows a very basic decision tree that should be used when starting a new application. The first decision is to select a class of optical indicators based on what is to be measured: VSD for membrane potential, CaSD for calcium concentration or another ion-sensitive indicator for concentration of other ions. Then the specific indicator must be selected. For VSDs it is largely a matter of selecting an absorbance versus fluorescence indicator, the desired spectral characteristics (based on available optical filters, light sources and tissue properties such as autofluorescence), and trial and error due to the variability in dye loading from preparation to preparation. For ion-sensitive dyes, one must also consider affinity and kinetics of the dye needed for the particular application as well as the spectral characteristics. Furthermore, for ion-sensitive dyes one must choose between selective loading of specific structures or bath-application; whereas, for the VSDs, only bath-application is commonly available, although see section “Voltage-sensitive Dyes”. The next step

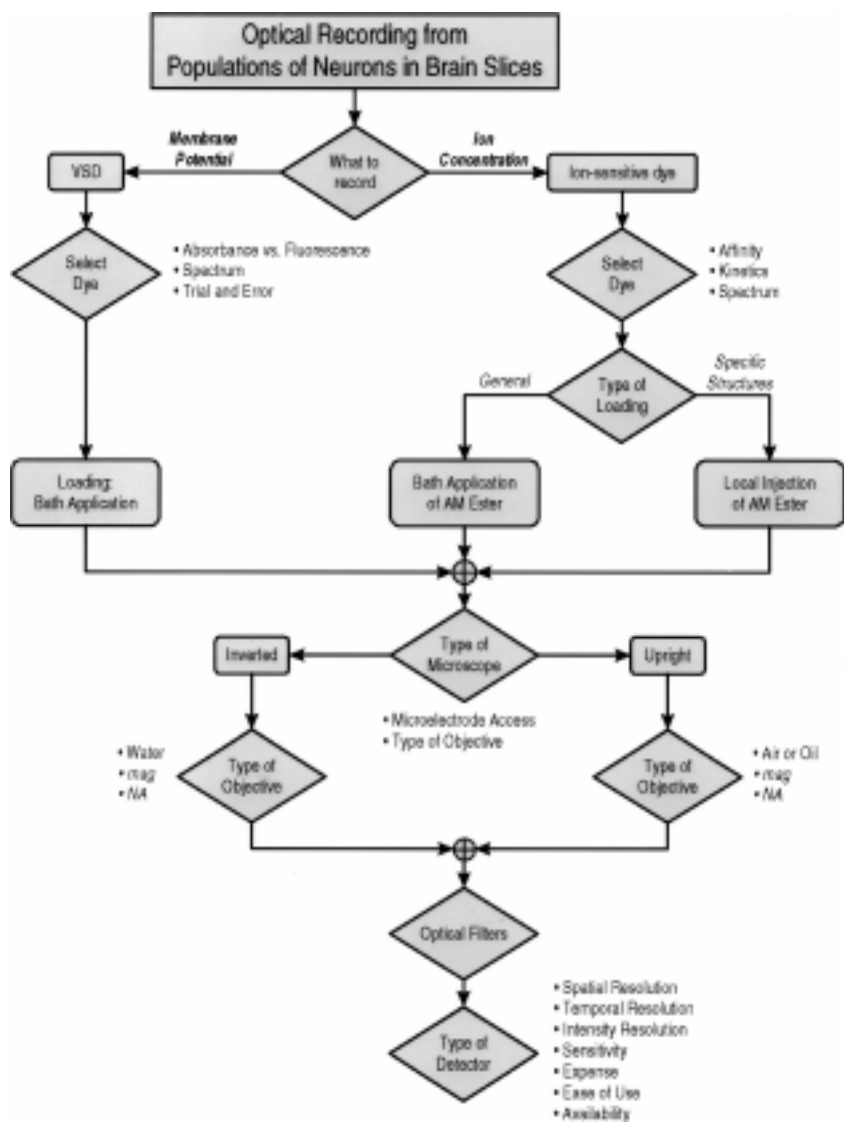


Fig. 5. Outline of experiment planning. The decisions involved in planning an optical recording experiment are illustrated. Next to the decision boxes (*diamonds*) are the various issues that should be considered in making that selection. See text for details.

is to select the type of microscope (upright or inverted) and objective. The relative advantages and disadvantages of different microscope configurations have already been discussed. For the objective lens, the main factors will be the type (air or oil for inverted and water for upright), the desired *mag* and *NA*, and the working distance (see Table 2). Optical filters should be selected based on the characteristics of the indicator. Lastly, the type of detector must be selected. All of the issues that were discussed previously need to be considered thoroughly before making a decision. In addition, we highly recommend that a single photodiode be used first to test the feasibility of the planned experiments, including the quality of indicator loading, size of signals, intensity of light reaching the detector (see Troubleshooting section for more details). Below, we give some specific examples of optical recording procedures that we have implemented after going through a decision process similar to that discussed here.

## ■ Materials

- Inverted microscope with epi-fluorescence capability (e.g., IM35 or Axiovert10, Zeiss); see section “Results” for the specific microscope objectives used.
- Light source: tungsten halogen lamp (12 V, 100 W, e.g., Xenophot HLX, Osram) or xenon burner (e.g., XBO 75W/2, Osram).
- Power supply for light source with RMS noise <0.01%: (e.g., ATE 75-8, Kepco, Flushing, NY) or battery-powered constant current source.
- Computer-controlled shutter (e.g., Uniblitz, Vincent, Rochester, NY).
- Photodetector: single photodiode, photodiode array or cooled CCD camera.
- Dyes and appropriate optical filters (see Table 1).
- Bath solution (in mM): NaCl 124, KCl 5, CaCl<sub>2</sub> 2, MgCl<sub>2</sub> 1.2, NaHCO<sub>3</sub> 26, D-glucose 10, saturated with 95% O<sub>2</sub>/5% CO<sub>2</sub>. All solutions should be bubbled constantly.
- DMSO (Sigma, St. Louis, MO), Pluronic acid (Molecular Probes, Eugene, OR).
- VSD staining chamber: small volume chamber with provision for staining solution access to both sides of the brain slice and for bubbling with 95% O<sub>2</sub>/5% CO<sub>2</sub> mixture. For example, a 5 cc syringe with the plunger removed and with the other end sealed with heat or silicone, containing a mesh (plastic or stretched nylon pantyhose) placed over a plastic ring of the appropriate size. For bubbling, a 20 to 25 gauge needle can be used.
- CaSD staining chamber: 35 mm plastic Petri dish with small hole in cover that is sealed with dental wax after passing 20 to 25 gauge needle. The needle should be angled such that the 95% O<sub>2</sub>/5% CO<sub>2</sub> mixture blows over the surface of the staining solution rather than in it. This is necessary because the CaSD staining solution contains pluronic acid, a detergent, and blowing gas directly into the solution leads to the formation of very large bubbles and foam.
- Recording chamber: a submersion chamber with a glass cover slip (#0) for the bottom. Chamber should have provisions for circulating solution, for holding the brain slice in place, and, if desired, for adjusting the temperature of the circulating solution (31–32°C for the experiments shown here).

## ■ Procedure

### Preparation of Hippocampal Slices

The procedure used in our laboratory to prepare transverse hippocampal slices is described briefly here; however, any procedure that gives viable slices may be used. The appropriate staining solution should be made before cutting brain slices.

1. Anesthetize the animals with methoxyflurane and quickly decapitate with a guillotine.
2. Remove the brain and place in ice-cold bath solution and allow to cool for ~3–5 min.
3. Dissect the hippocampi free from the remainder of the brain.
4. Mount hippocampi on stage of a vibrating tissue slicer (e.g., Vibratome 1000, TPI) and cut 400 μm slices from the middle 1/3 of the hippocampus.
5. Store slices at room temperature in bath solution for at least 1 h before staining, except when staining with bath-application of CaSD, in which case slices may be transferred to the staining solution immediately.

### Dye Loading

1. Prepare stock solution of RH-414: 4 mM in distilled water. This solution can be stored in the freezer for up to several months.

### VSD Loading

2. On day of experiment, add 10–20  $\mu$ l of RH-414 stock solution to 4 ml of bathing solution to obtain staining solution (bathing solution with 25–50  $\mu$ M RH-414). Place staining solution in VSD staining chamber with bubbling needle.
3. Transfer one slice to staining chamber. Stain for 15 min; bubble solution at a rate that will just not move the slices.
4. Wash slice in 20 ml of bath solution for 15–30 min before transferring to recording chamber on stage of microscope.

### CaSD Loading **Bath-application**

1. Prepare solution of 75% DMSO and 25% pluronic acid by weight. Gentle heating will be required to get pluronic acid into solution. Solution may be stored at room temperature and used for up to 1 week. It may be necessary to gently reheat the solution on subsequent days. After heating this solution, allow it to cool to room temperature before using.
2. Add 10  $\mu$ l of DMSO/pluronic acid solution to 50  $\mu$ g container of Calcium Orange-AM. Let solution stand for 30 min at room temperature.
3. Immediately after cutting hippocampal slices, add 1 ml of bathing solution to container. Shake vigorously to mix.
4. Sonicate for 5–10 min at highest setting.
5. Transfer above solution and 4–5 brain slices to the CaSD staining chamber.
6. Loosely seal with Parafilm and start blowing O<sub>2</sub>/CO<sub>2</sub> mixture over staining solution at the highest flow rate that does not cause the slices to move.
7. Stain for 3–3.5 h at 30 °C.
8. Unseal container, add 2 ml bath solution and reseal until slices are needed. Slices may be kept in this holding solution for several hours.
9. Wash one slice in 20 ml of bath solution for 15–30 min before transferring to recording chamber on stage of microscope.

### Selective Loading

1. Prepare 75% DMSO/25% pluronic acid solution as described in step 1 of section on bath-application of CaSD.
2. Dissolve 5  $\mu$ l DMSO/pluronic acid solution to 50  $\mu$ g container of the CaSD-AM (Fura-2-AM or Fura-2-AM). Let solution stand for 30 min at room temperature.
3. Add 50  $\mu$ l bath solution to container. Shake vigorously to mix.
4. Sonicate for 5–10 min at highest setting.
5. Prepare micropipette (~2  $\mu$ m tip diameter).
6. Load tip of micropipette with small amount of dye solution by gently applying suction to back of micropipette with a syringe connected to plastic tubing.
7. At least one hour after cutting brain slices, transfer one slice to recording chamber on stage of microscope.
8. Pressure-inject (~10 p.s.i., 20 msec, 5–10 pulses) a small amount of the dye solution (<<1  $\mu$ l) into the appropriate axonal tract, 0.5–1 mm away from the recording site (e.g., Schaffer collaterals for loading presynaptic terminals of area CA3 pyramidal cells, see Fig. 6, or alveus for loading postsynaptic structures of area CA1 pyramidal cells).

**Note:** best results are obtained when the direction of fluid flow in the recording chamber is such that any excess dye at the injection site is carried away from the recording site.

9. Recording may commence ~1 h after injection when fluorescence emerges in the recording area.

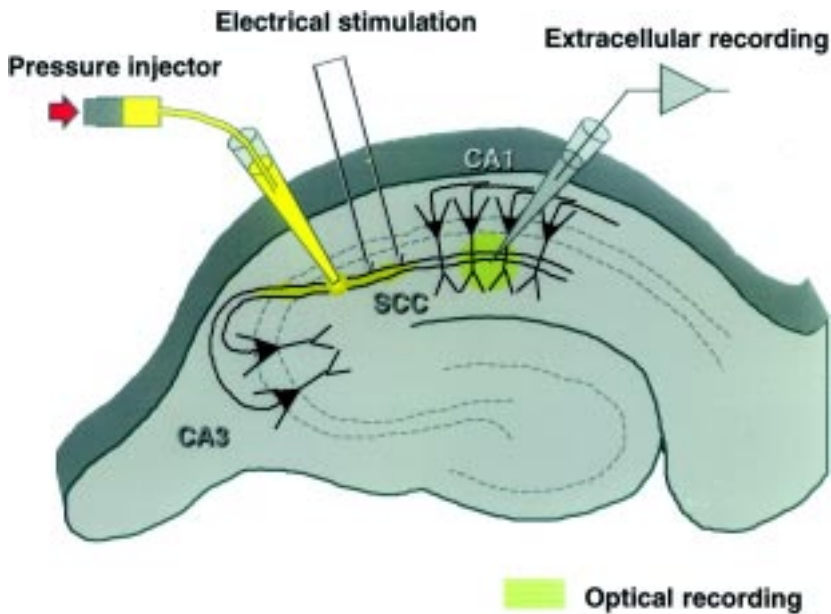


Fig. 6. Technique for selective loading of CaSD. A small amount of CaSD ( $\sim 1$  mM of AM ester in DMSO/pluronic solution) is pressure-injected into *str. radiatum* of area CA1, which is the location of CA3 pyramidal cell axons (Schaffer collateral/commissural pathway, SCC). Indicator is taken up, trapped intracellularly by esterases and diffuses within the axons, filling presynaptic terminals at the recording site. Approximate locations of stimulation and recording electrodes are shown.

### Optical Recording Procedure

Below we describe the specifics of the procedures for recording evoked or spontaneous signals from slices loaded using the various protocols described above. Regardless of the specifics of the experiments, there are several things that should be done in any optical recording experiment. First, the autofluorescence of the tissue should be measured; as discussed previously, this is especially important when using indicators that are excited by short wavelengths of light. In the case of slices where specific structures are loaded by injection of CaSD into axonal tracts, autofluorescence may be measured within the same slice in a region analogous to the recording area that has not been loaded or in the recording area itself prior to loading. In the case where the brain slices are loaded by bath-application of the indicator, autofluorescence should be measured in an analogous area in another brain slice from the same animal. It is important that the illumination intensity be the same during the measurement of the autofluorescence and during the actual recording period.

Another measurement that should be made during each experiment is a bleaching trace. During exposure to light, molecules of optical indicator are bleached, i.e., lose their fluorescence. It is not clear if these molecules are actually destroyed or if they are put into a state where they are temporarily unable to fluoresce. Regardless of the exact mechanism, bleaching is a mono-exponential process for which it is easy to compensate. The easiest bleaching correction procedure requires the recording of a trace in a period without activity – neither evoked nor spontaneous. The parameters for collecting the bleaching trace (digitization rate, duration, time when shutter is opened) should be exactly the same as for collecting the data trace. Another possibility is that, because bleaching is an exponential process, if the shutter is opened for a sufficiently long period

of time before the actual data collection is started, then bleaching will have nearly reached a steady state during the data collection. This latter technique is useful when recording spontaneous activity.

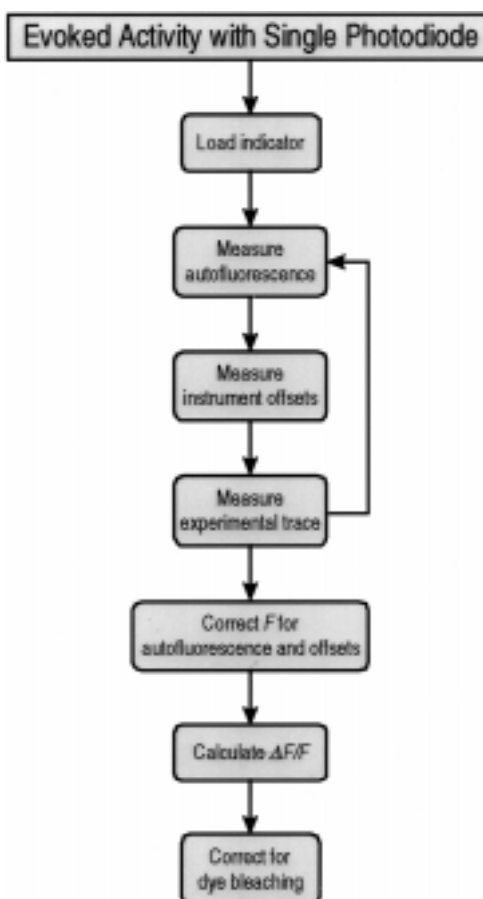
#### Evoked Activity with Single Photodiode

For recording evoked activity with a single photodiode, the recording procedure is relatively straightforward. We typically use an oil-immersion objective (Achromplan 50 $\times$ , NA 0.9, Zeiss). For digitization of data and providing the digital lines used to control the shutter and electrical stimulator, we use a multipurpose I/O card (12-bit, 50kHz, DAS-50, Keithley). The signal from a conventional microelectrode used to record the extracellular field potential and the signal from the single photodiode are both digitized by this card. Fig. 7 illustrates the steps involved in a typical experiment. First the appropriate autofluorescence is measured.

#### Evoked Activity with PDM

For recording activity with the photodiode matrix, we typically use a 10 $\times$ , NA 0.5 objective (Zeiss). For digitization of data and providing the digital lines used to control the PDM amplifier, shutter and electrical stimulator, we use a multipurpose I/O card (Flash 12, Strawberry Tree). The A/D converter on this card is 8 channels, 12-bit, 400kHz with 256k sample on-board memory; it also has 8 TTL I/O lines and a 2-channel D/A converter. The field potential recorded by a conventional microelectrode is fed into the PDM amplifier and is multiplexed with all the optical channels as shown in Fig. 4. The steps involved in a typical experiment are illustrated in Fig. 8. For the reasons discussed

Fig. 7. Procedure for recording evoked activity with single PD. See text for details.



previously, separate AC and DC measurements were necessary. Because the optical indicators we typically used with the PDM were those excited by longer wavelengths, it was unnecessary to perform an autofluorescence correction as the autofluorescence was much lower than the level of offset in the amplifier.

The same hardware and basic procedures are used to record spontaneous activity with the PDM as for evoked activity. The main additional challenge in recording spontaneous activity is the lack of an event on which to trigger data collection. Continuous recording, which is often used to record spontaneous activity with microelectrodes, is not an option due to the large amount of data involved (>100 channels). We have employed two procedures for recording spontaneous activity with PDMs. The first procedure uses software which relies on luck to capture spontaneous activity (Colom and Saggau 1994; Sinha et al. 1995): data epochs of a defined length are collected and displayed; when the user sees an event of interest, data collection is stopped and the last epoch is saved. This procedure is sufficient for recording relatively frequent events, i.e., those occurring at frequencies faster than 0.2 Hz; however, with this technique it is very difficult to reliably record more infrequent events.

A slight modification of this recording procedure allows for reliable recording of events occurring at frequencies < 0.05 Hz. A flow chart of this modified procedure is

Spontaneous Activity  
with PDM

Fig. 8. Procedure for recording evoked activity with PDM. See text for details.

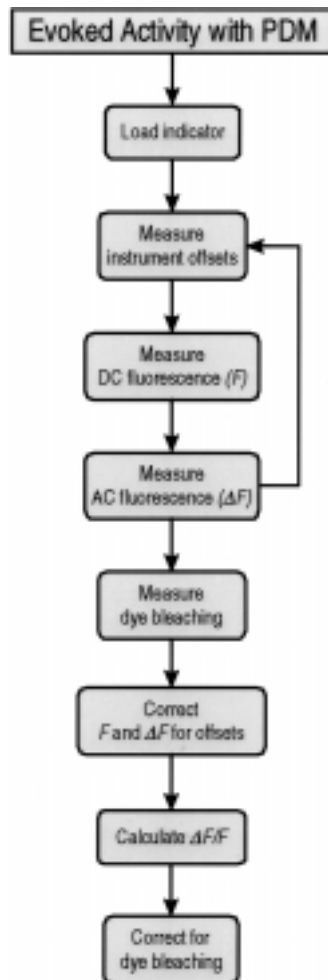
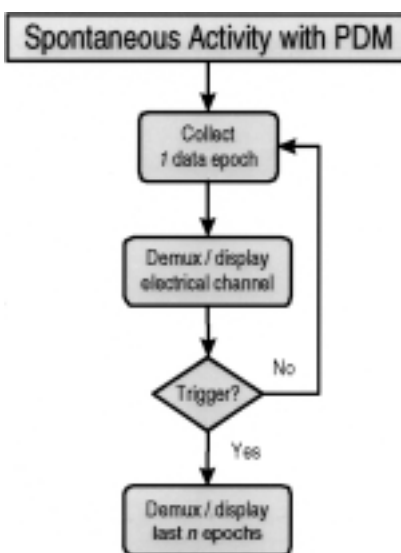


Fig. 9. Procedure for recording spontaneous activity with PDM. See text for details.



shown in Fig. 9. An epoch of data (typically 0.5–1 sec) is collected, and only the electrical channel is demultiplexed and displayed. This process is repeated until the user observes spontaneous activity and triggers the computer; the last  $n$  epochs collected previous to the trigger (typically 2–3) are then demultiplexed, displayed and available for further manipulation and storage.

### Processing of Optical Data

The first step in processing the optical data is to correct for any autofluorescence and instrumentation offsets. In the case of a single photodiode, these quantities are simply subtracted from all points in the optical trace; in the case of the PDM, they are subtracted from the DC fluorescence, which represents the static fluorescence. All optical signals are displayed as change in fluorescence divided by resting fluorescence ( $\Delta F/F$ ). This corrects for variations in dye concentration, in illumination intensity and in the sensitivity of the individual detector elements. For a single photodiode, resting fluorescence ( $F$ ) is simply the average fluorescence in the portion of the data trace before any activity is observed, i.e., before the application of any stimuli; change in fluorescence ( $\Delta F$ ) is obtained by subtracting  $F$  from each data point in the trace. For the PDM, the DC fluorescence is the resting fluorescence ( $F$ ) and the AC trace is the change in fluorescence ( $\Delta F$ ). For the CaSD an increase in  $\Delta F/F$  corresponds to an increase in  $[Ca^{2+}]_i$ . For the VSD a decrease in  $\Delta F/F$  corresponds to depolarization; therefore, all VSD traces are inverted so that a depolarization corresponds to an upward deflection.

For both types of detectors, bleaching correction is performed by first calculating  $\Delta F/F$  for both the data and bleaching traces and then subtracting, point by point or in the case of the PDM, element by element, the bleaching trace from the data trace.

For quantification of optical signals, we use two different measurements. For both the VSD and CaSD, the amplitude of the signal can be used. For the VSD alone, another quantity, the mean window amplitude (MWA; Albowitz and Kuhnt 1995) is also a useful measure. The MWA is simply the mean value of the VSD signal during a defined time window. Unlike the amplitude, MWA reflects changes in duration of activity as well as its maximal amplitude. Also, for small signals, it has the additional advantage of reducing the effect of noise: the contribution of noise components with periods smaller than the period of time over which the MWA is calculated will be reduced in calculating this

time-averaged value. It is important to note that calculating the MWA for a CaSD signal is relatively meaningless as the duration of the CaSD signal is affected by the kinetics of the indicator in addition to the duration of the calcium concentration transient. A quantity that is useful for CaSD signals is the amplitude of the first derivative of the signal: if the CaSD signal is proportional to  $[Ca^{2+}]_i$  and no significant calcium release from internal stores occurs, then the derivative is proportional to the calcium influx. Furthermore, if a dye with fast kinetics is used, i.e., one with a low affinity for  $Ca^{2+}$ , then the duration of this derivative is approximately the duration of the calcium influx (for more details, see Sinha et al. 1997).

## ■ Results

Using the techniques described above, we have conducted a number of investigations in the hippocampal slice looking at different aspects of synaptic transmission, modulation of transmitter release, plasticity and epileptiform activity in the hippocampal slice (Wu and Saggau 1994a,b, 1995, 1997; Qian and Saggau 1997a,b; Colom and Saggau 1994; Sinha et al. 1995, 1997). Below we present examples taken from these investigations that illustrate the various techniques. For more examples and details, the reader should refer to the individual articles.

### Evoked Signals with Selective Loading of CaSD

Fig. 10A illustrates an experiment where the CaSD Fura-2 was selectively loaded into presynaptic terminals of area CA3 pyramidal cells by pressure injecting into the Schaffer collaterals (see Fig. 6). Signals were recorded in *stratum radiatum* of area CA1. Selective recording is insured by the fact that only the axons of the CA3 pyramidal cells travel from the site of injection to the site of recording; some interneurons and glia may also have processes which span this region, but they are vastly outnumbered by the axons. The selectivity of the loading can be illustrated by blocking all postsynaptic activity with the glutamate receptor antagonists CNQX and D-APV; these antagonists completely block the postsynaptic response but do not affect the CaSD signal, confirming its presynaptic origin.

The dependence of the CaSD signal on the  $K_d$  (and  $k_{on}$  and  $k_{off}$ ) is illustrated in Fig. 10B,C, which shows the same calcium concentration transient measured with a high affinity CaSD (Fura-2) and a low affinity CaSD (Fura-2ra). Both indicators are measuring the calcium transient evoked in CA3-CA1 presynaptic terminals by a single action potential. The faster kinetics of the low affinity indicator, Fura-2ra, are apparent. A combined modeling and experimental study (Sinha et al. 1997) demonstrated that while the high affinity indicator, Fura-2, may be locally saturated by the high local  $[Ca^{2+}]_i$  near the plasma membrane after a single action potential, its overall amplitude is still proportional to this local concentration. Thus, Fura-2 can be used to investigate presynaptic calcium transients evoked by single action potentials. However, for calcium transients evoked by multiple action potentials, it is more prudent to use a lower affinity indicator such as Fura-2ra.

Our laboratory has used this technique extensively to investigate which calcium channels are involved in transmitter release at the CA3-CA1 synapse, how presynaptic calcium influx is altered during synaptic plasticity, and the role of presynaptic calcium in modulation of transmitter release (for review, see Wu and Saggau 1997). We have also used this technique to specifically load other structures in the hippocampal slice; furthermore, others have used a similar technique (using local perfusion with CaSD rather than injection) to specifically load structures in hippocampal and cerebellar slices. The

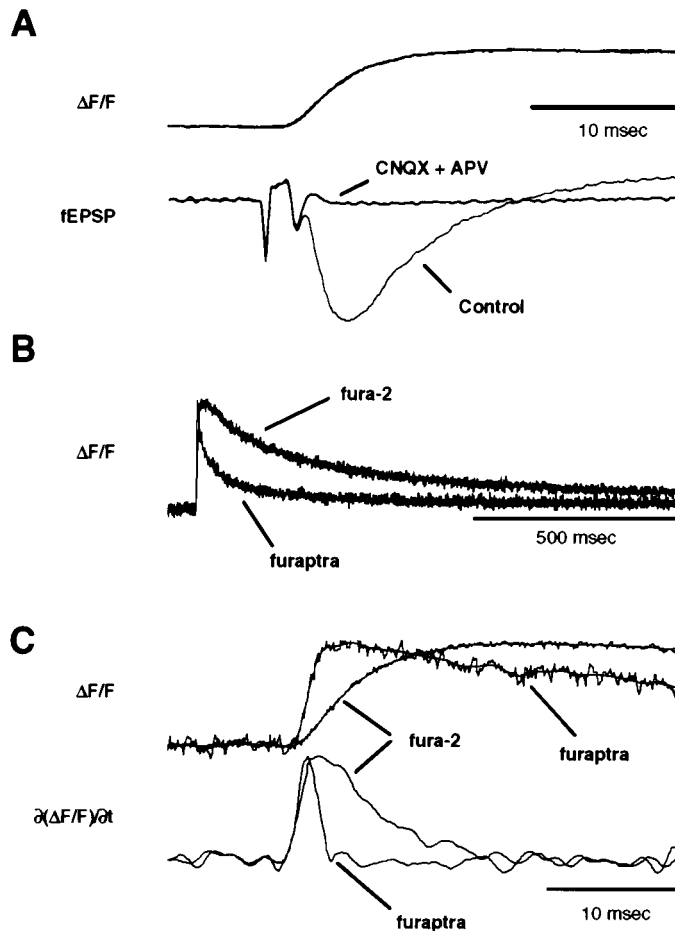


Fig. 10. CaSD transients from selectively loaded presynaptic terminals recorded with a single photodiode. Presynaptic axons and terminals of CA3 pyramidal cells were loaded with the CaSD Fura-2, using the technique described in Fig. 6. **A.** Overlaid fEPSPs and CaSD transients evoked by a single stimulus in area CA1 under control conditions and after the application of glutamate receptor antagonists (CNQX, 10  $\mu$ M, + D-APV, 25  $\mu$ M) to block postsynaptic activity. Blocking postsynaptic activity does not alter the CaSD signal, indicating a presynaptic origin. **B.** Comparison of presynaptic calcium transients measured with a low affinity (Fura-2) and a high affinity (Fura-2) CaSD. CaSDs were loaded as described in A. Normalized transients evoked by a single electrical stimulus are shown. **C.** The same transients on a faster time scale (*top*) and the first derivative of the calcium transients (calcium influx, *bottom*). The low affinity indicator allows for the observation of more rapid transients with less distortion than the high affinity indicator.

postsynaptic CA1 pyramidal cells can be selectively loaded by injecting CaSD into the alveus (Regehr and Tank 1991; Wu and Saggau 1994a). Presynaptic mossy fiber terminals in area CA3 can be loaded by injecting CaSD into the hilus (Regehr and Tank 1994; Qian and Saggau, unpublished observation). Also, parallel fiber presynaptic terminals in the cerebellum can be selectively loaded using this technique (Mintz et al. 1995).

#### Evoked Signals with Bath-applied CaSD

Fig. 11 shows an experiment where the CaSD Calcium Orange was bath-applied to a hippocampal slice, and calcium transients evoked by a single electrical stimulus applied to

the Schaffer collaterals were recorded in area CA1. Because the indicator was bath-applied, it was non-selectively loaded into the various pre- and postsynaptic neuronal structures. This can be illustrated by applying the ionotropic glutamate receptor antagonists CNQX and D-APV to block the postsynaptic response without altering the presynaptic activity. The relative contributions of the various cellular structures to the overall CaSD signal depends on two main factors: (1) the size of the change in  $[Ca^{2+}]_i$  in those structures and (2) the volume of the structures:

$$CaSD = \sum (\Delta[Ca^{2+}]_i \times Volume_i)$$

The second factor is due to the fact that the number of indicator molecules in a particular structure is roughly proportional to its volume. For a more detailed discussion of the contribution of different cellular elements to the CaSD signal see Sinha et al (1995).

Fig. 11C illustrates how this technique can be used to obtain information about the spatio-temporal characteristics of neuronal activity. CaSD signals are first seen in the dendritic regions, the location of the presynaptic terminals, closest to the site of stimu-

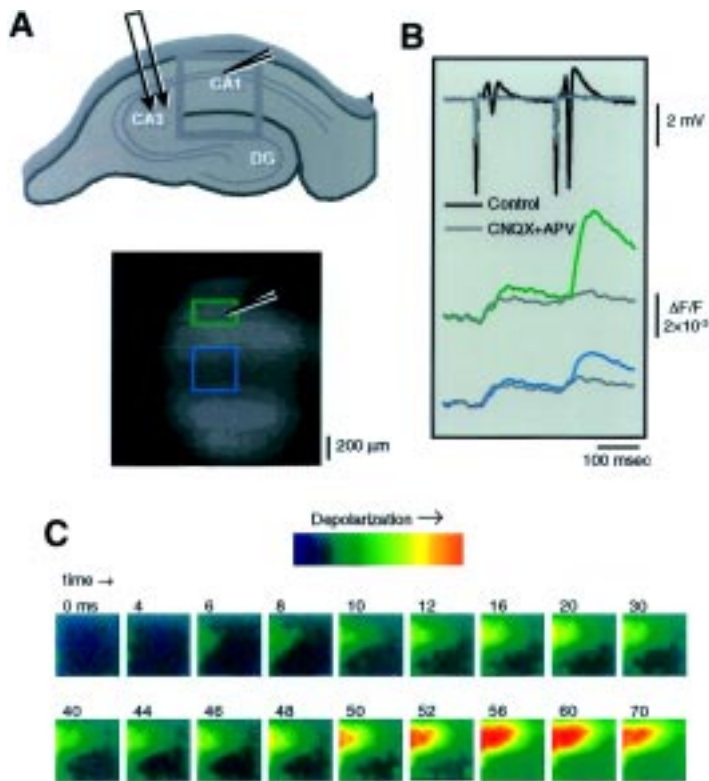


Fig. 11. Evoked CaSD transients recorded with a PDM. The CaSD Calcium Orange was bath-applied as described in section “CaSD Loading”. Signals evoked by stimulating the Schaffer collaterals were recorded in area CA1 with a  $10 \times 10$  PDM as described in Fig. 8 A. Schematic of brain slice showing recording area and positions of recording and stimulation electrodes (*top*); CCD image of recording area indicating groups of PDM elements (framed) from which data is shown in B and C (*bottom*). Green frame covers *str. pyramidale*; blue frame covers *str. radiatum*. B. Evoked activity in response to pair of electrical stimuli recorded under control conditions and in the presence of CNQX ( $10 \mu M$ ) + D-APV ( $25 \mu M$ ). Field electrode recordings (*top*) and sample CaSD signals are shown (*bottom*). C. Time lapse illustrating the spatio-temporal nature of the CaSD signals recorded under control conditions. Time 0 corresponds to the first stimulus; 60 msec corresponds to the second stimulus.

lation (to the left of the region shown in the figure). They then spread across the brain slice away from the site of stimulation and into the cell body layer, *stratum pyramidale*, the location of the postsynaptic cell bodies. While there is significant loading of CaSD into glial cells (Albowitz et al. 1997), changes in  $[Ca^{2+}]_i$  in glial cells tend to occur on much slower time scales, thus contributing little to the transients shown here.

### Spontaneous Epileptiform Activity Recorded with Bath-applied VSD

Optical recording techniques are extremely well suited for investigations of the spatio-temporal characteristics of complex activity in neuronal populations, such as spontaneous epileptiform activity. We have previously used this technique to extensively investigate different aspects of spontaneous interictal epileptiform activity in the hippocampal slice (Colom and Saggau 1994; Sinha et al. 1995, 1996). Fig. 12 shows a sample experiment where synchronized activity in the hippocampal interneuronal network was recorded using the VSD RH-414 and a PDM. This activity occurs spontaneously in the presence of the  $K^+$  channel antagonist 4-aminopyridine (4-AP, 100  $\mu$ M) and can be isolated from spontaneous interictal epileptiform activity by the application of the ionotropic glutamate receptor antagonist CNQX and D-APV (Michelson and Wong 1994; Sinha et al. 1996). This activity is mediated by GABA<sub>A</sub> receptor-mediated depolarizing responses among interneurons. Using this technique has allowed us to investigate the spatio-temporal characteristics of this activity and to compare it to spontaneous interictal epileptiform activity (Sinha et al. 1996). We are currently in the process of further characterizing this activity and investigating the specific types of interneurons involved in generating it and the mechanisms responsible.

As discussed above for  $[Ca^{2+}]_i$  and CaSDs, the activity recorded by a single element of the PDM when using a VSD actually represents a weighted average of the membrane potential transients in all the structures located in the recording area covered by that detector element. For VSDs, which remain on the surface of cells, this weight is the surface area of the structures:

$$VSD = \sum (\Delta V_{m,i} \times \text{SurfaceArea}_i)$$

For a more detailed discussion of the contribution of various cellular structures to the VSD signal, see Sinha et al. (1995).

Because the VSD signals represent an average of the membrane potential in multiple structures, the possibility exists that if some of these structures are hyperpolarized while others are depolarized, their activities may cancel each other out to give the false impression of the absence of activity. This is not as big a concern with CaSD signals because few physiological manipulations cause a rapid decrease in  $[Ca^{2+}]_i$  from resting levels. Another important fact to keep in mind is that due to the relatively slow nature of the activity being recorded, the AC coupling constant of the PDM (~100 msec) may actually affect the signals. This problem could be avoided by using an A/D converter with sufficient intensity resolution to allow for recording only in DC-coupled mode, as with the single photodiode. Note: the sensitivity of this technique is not sufficient to record spontaneous activity in individual neurons; the activity must be occurring in a population of neurons.

### ■ Troubleshoot

Optical recording is a technically demanding endeavor and a systematic approach is essential. This is as true for the initial planning and implementation as it is for troubleshooting of the techniques.

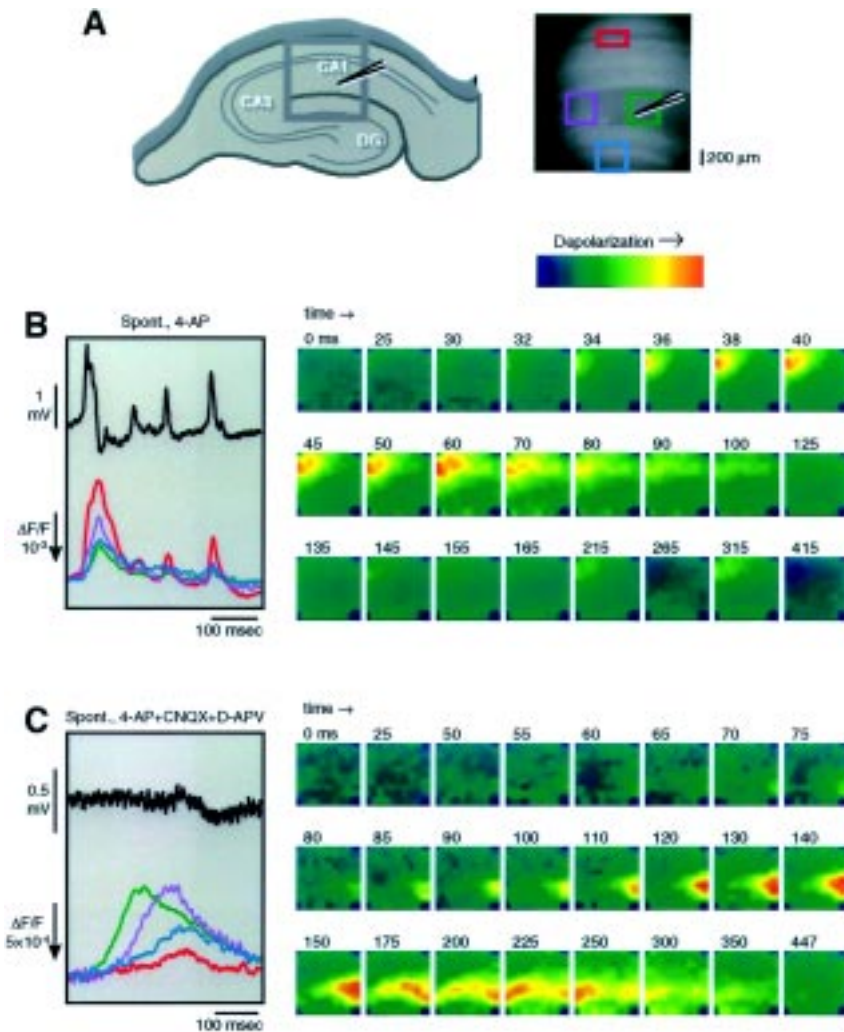


**Fig. 12.** VSD transients associated with spontaneous epileptiform activity recorded with a PDM. The VSD RH-414 was loaded by bath-application as described in section “VSD Loading”; spontaneous synchronized activity was recorded with a  $10 \times 10$  PDM as described in Fig. 9. **A.** Schematic of brain slice showing recording area and position of recording electrode (*left*); CCD image of recording area indicating groups of PDM elements (framed) from which data is shown in B and C (*right*). **B.** Spontaneous epileptiform activity recorded in  $100 \mu\text{M}$  4-AP. Field electrode recording and sample VSD signals are shown (*left*) along with a time lapse illustrating the spatio-temporal nature of the activity (*right*; time 0 corresponds to the beginning of the traces shown on the left). The activity originated in area CA3 and spread across the CA1; it was confined mainly to *str. pyramidale* and proximal dendritic regions. **C.** Spontaneous synchronized interneuronal activity recorded in 4-AP +  $10 \mu\text{M}$  CNQX +  $25 \mu\text{M}$  D-APV. This activity originated in the subicular side of area CA1 and spread towards CA3; it was largest in the distal apical dendritic region.

A step that can greatly aid in troubleshooting is to start with a single photodiode as the photodetector. In addition to the advantages discussed previously, the output of a single photodiode with its amplifier can be directly monitored with an oscilloscope. This removes the added complexity of the data acquisition hardware, which is only necessary for later processing, i.e., signal averaging, and storage of data for a single photodiode (with CCD cameras or PDMs it is much more difficult or even impossible to monitor the data without the data collection hardware). Thus, we highly recommend that the

first step should be to fine tune all other aspects of the experimental design (indicator loading, light source noise, optical filter selection, data collection hardware) using a single photodiode. Once this has been accomplished, then the desired photodetector can replace the single photodiode. The only troubleshooting that should then remain will involve the new photodetector and/or its interface with the data acquisition hardware.

– Test Equipment

A relatively simple way of testing the photodetector and data collection hardware and procedures is to use a light-emitting diode (LED) powered by a function generator as a test preparation. Most function generators have the capability to output a small AC component (e.g., a square wave) superimposed on a larger DC component. An LED powered by such a waveform will mimic a typical optical signal: a small  $\Delta F$  with a relatively large  $F$ . This method can easily generate a signal with a fractional change on the order of  $10^{-2}$  (generation of smaller fractional changes requires a custom-made test circuit with a very stable power supply). Such a test preparation allows one to test the entire detector and data acquisition hardware without the added complications that a biological preparation introduces.

– Indicator Loading

There are several aspects of indicator loading that need to be optimized and checked in order to obtain the best signals for a given experimental design. The optimal concentration and the period of incubation are typically different for different indicators and preparations. The numbers given in the protocols in this chapter are those we have found to be optimal for the specific applications and to provide a good starting range; however, the user should always try a range of values. It should be noted that using the highest indicator concentration for the longest incubation period might provide the highest fluorescence but not necessarily the best signal. This can be due to nonspecific staining of structures that are not of interest and, in the case of membrane-permeable AM esters, loading of subcellular structures (e.g., endoplasmic reticulum or mitochondria). As mentioned in section “Voltage-sensitive Dyes”, it is also important to try different indicators to determine which is best suited for a particular preparation. In the case of AM esters, it might be worthwhile to try brain slices from younger animals to obtain improved loading.

– Origin of Signals

Another aspect of indicator loading that is very important when recording from populations of neurons in brain slices is the location of the loaded indicator and, thus, where the optical signals are originating. For indicator that has been bath-applied this is mainly a matter of determining whether the signals are from neuronal or glial structures. The time course of signals can be useful in this respect: glial signals tend to be much slower and/or smaller than neuronal signals (Prince et al. 1973; Dani et al. 1992) and generally require more intense stimuli (Porter and McCarthy 1996). Also, for fluorescent indicators, confocal microscopy can be used to determine the indicator location (Albowitz et al. 1997). In the case where the attempt is made to load specific structures in a slice, one can use pharmacological tools (e.g., blocking postsynaptic activity to determine if signals are originating for pre- or postsynaptic structures) or selective activation of a group of cells.

– Artifactual Signals

Once an optical signal has been obtained, it is important to determine whether it is an actual indicator signal or an artifact. The two main sources of artifacts that may mimic an indicator signal are movement and intrinsic signals. Because of the small size of optical indicator signals, very small movements in the preparation can lead to changes in the light seen by the photodetector that are on the same order of magnitude as the optical signal or even larger. In addition, as discussed in Chapter 34 (Grinvald et al.), the intrinsic optical properties of neuronal tissue change with activity. In

order to determine if the recorded signals are actually from the indicator, several approaches can be taken. One is to determine the spectral properties of the signal, as movement artifacts and intrinsic optical signals are relatively wavelength-independent, whereas optical indicator signals are not. Furthermore, with some optical indicators, the direction of the voltage- or calcium-dependent change of the optical signal will actually vary with the wavelength (e.g., VSD RH-155 or CaSD Fura-2); artifactual signals will not do this. Another way of distinguishing between actual signals and artifacts is to compare recordings from stained and unstained preparations.

– Indicator Toxicity

Although optical recording techniques are generally much less invasive than conventional approaches, the presence of an indicator may still affect the preparation. One obvious effect is the possibility of indicator toxicity; while this was a more significant problem with earlier indicators, it is still an important factor to keep in mind. Actually testing for toxicity can be as simple as monitoring the effect of the indicator on electrical responses such as field potentials. If the indicator is noted to significantly deteriorate the health of the preparations, several options are available such as reducing the indicator concentration if possible, or trying another indicator. Also, because the toxicity of most indicators, specially the VSDs, is related to substances produced by intense illumination in the presence of oxygen, reducing the amount of light exposure will typically reduce toxicity. Unfortunately, the use of antioxidants or even removal of oxygen from the bathing solution is not a viable option for mammalian brain slices.

– Buffering by Indicators

Aside from toxicity, optical indicators can also alter properties of the preparation. This is specially true for ion-sensitive indicators, which act as buffers for the ion that they bind and thus can alter the concentration and dynamics of that ion. In general, the higher the concentration of the indicator and the higher its affinity for the ion, the more likely it is to have such an effect. This is very important to keep in mind when interpreting optical signals from CaSDs. The extent to which this is a factor can be determined by varying either the concentration of the indicator (difficult to do when loading by bath-application) or to use an indicator with a lower affinity (e.g., Fura-2 instead of Fura-2).

– Signal-to-Noise Ratio

Because of the small size of most optical signals, obtaining a sufficient signal-to-noise ratio (SNR) is frequently a problem. Noise in an optical recording system can be classified into one of three categories: dark noise, source noise and shot noise. Dark noise is present even in the absence of light; it is the noise that is intrinsic to recording apparatus and is independent of the amount of light:

$$N_{dark} = \text{const.}$$

Source noise is due to fluctuations in the intensity of the light emanating from the light source. It can be the result of noise in the power supply, noise intrinsic to the light source, or noise that is somehow introduced in the light path (e.g., motion artifact). Source noise is proportional to the amount of light:

$$N_{source} \propto I$$

Shot noise is due to the quantal nature of light. It is proportional to the square root of the light intensity:

$$N_{shot} \propto \sqrt{I}$$

The first step in determining how to improve SNR is to identify the predominant source of the noise. This can be done by determining how noise varies with light inten-

sity: invariant ( $N_{dark}$ ), proportional ( $N_{source}$ ) or exponential ( $N_{shot}$ ). Because the optical signal is proportional to light intensity, the effect of varying the light intensity on  $SNR$  for these various types of noise are:

$$SNR_{dark} \propto I$$

$$SNR_{source} = \text{const.}$$

$$SNR_{shot} \propto \sqrt{I}$$

Thus if the limiting noise is either  $N_{dark}$  or  $N_{shot}$ , increasing the intensity of illumination will improve  $SNR$ . However, if  $N_{source}$  is the limiting noise, then only decreasing  $N_{source}$  (i.e., using a more stable light source and/or power supply) will improve  $SNR$ . A simple approach to improving  $SNR$  is to average signals. This can refer to taking the average of a number of trials (temporal averaging) or, in the case of spatially-resolving photodetectors, the average of several photodetector elements (spatial averaging). In both cases, the improvement in  $SNR$  obtained by averaging is:

$$SNR \propto \sqrt{n}$$

where  $n$  is the number of trials or elements that are averaged.

## ■ Comments

Optical recording techniques are powerful tools in cellular physiology. They provide the means for studies that would not be feasible with more conventional approaches, such as using micropipettes. In addition, they often offer an elegant approach to problems that may be very difficult to address with other techniques. In this chapter we have attempted to cover the basic issues involved in optically recording from populations of neurons in brain slices. Optical recording is a very broad and constantly growing field; even the variety of specific examples that we have shown from our own work can only provide a limited picture of the vast array of specific techniques and applications. However, the basic issues we have discussed are generally applicable and should provide a good starting point for anyone interested in using optical recording techniques to record from populations of neurons. Because of the large body of literature available in this field and because of the extremely rapid rate with which new techniques, indicators and hardware are being developed, we highly recommend that the next step after reading this article should be to scour the literature for examples that closely match the specific application. Chances are someone has at least tried it.

**Acknowledgement:** This work was supported in part by grants from NIMH MH 10491 (S.R.S.), NSF IBN-9723871 (P.S.) and NIH NS33147 (P.S.). We are grateful to L.G. Wu and Dr. J. Qian for their contributions to some of the reviewed techniques and studies. We also gratefully acknowledge the excellent technical assistance provided by Dr. S.S. Patel in various aspects of this project.

## ■ References

- Albowitz B, Konig P, Kuhnt U (1997) Spatio-temporal distribution of intracellular calcium transients during epileptiform activity in guinea pig hippocampal slices. *J Neurophysiol* 77:491–501.
- Antic S, Major G, Chen WR, Wuskel J, Loew L, Zecevic D (1997) Fast voltage-sensitive dye recording of membrane potential changes at multiple sites on an individual nerve cell in rat cortical slice. *Biol Bull* 193:261.
- Breckenridge LJ, Wilson RJA, Connolly P, Curtis ASG, Dow JAT, Blackshaw SE, Wilkinson CDW (1995) Advantages of using microfabricated extracellular electrodes for *in vitro* neuronal recordings. *J Neurosci Res* 42:266–276
- Colom LV, Saggau P (1994) Spontaneous interictal-like activity originates in multiple areas of the CA2-CA3 region of hippocampal slices. *J Neurophysiol* 71:1574–1585
- Dani JW, Chernjavsky A, Smith SJ (1992) Neuronal activity triggers calcium waves in hippocampal astrocyte networks. *Neuron* 8:429–440
- Denk, W. and Svoboda, K. (1997) Photon upmanship: Why multiphoton imaging is more than a gimmick. *Neuron* 18:351.
- Grynkiewicz G, Poenie M, Tsien RY (1985) A new generation of  $Ca^{2+}$  indicators with greatly improved fluorescence properties. *J Biol Chem* 260:3440–3450
- Haugland, RP (1996) Handbook of fluorescent probes and research chemicals, Molecular Probes, Eugene, OR
- Michelson HB, Wong RKS (1994) Synchronization of inhibitory neurones in the guinea pig hippocampus *in vitro*. *J Physiol (Lond)* 477:35–45
- Minta A, Kao JPY, Tsien RY (1989) Fluorescent indicators for cytosolic calcium based on rhodamine and fluorescein chromophores. *J Biol Chem* 265:8171–8178
- Mintz IM, Sabatini BL, Regehr WG (1995) Calcium control of transmitter release at a cerebellar synapse. *Neuron* 15:675–688
- Porter JT, McCarthy KD (1996) Hippocampal astrocytes *in situ* respond to glutamate released from synaptic terminals. *J Neurosci* 16:5073–5081
- Prince DA, Lux HD, Neher E (1973) Measurement of extracellular potassium activity in cat cortex. *Brain Res* 50:489–495
- Qian JQ, Colmers WF, Saggau P (1997) Inhibition of synaptic transmission by neuropeptide Y in rat hippocampal area CA1: modulation of presynaptic  $Ca^{2+}$  entry. *J Neurosci* 17:8169–8177
- Qian JQ, Saggau P (1997) Presynaptic inhibition of synaptic transmission in the rat hippocampus by activation of muscarinic receptors: involvement of presynaptic calcium influx. *Brit J Pharm* 122:511–519
- Regehr WG, Delaney KR, Tank WD (1994) The role of presynaptic calcium in short-term enhancement at the hippocampal mossy fiber synapse. *J Neurosci* 14:523–537
- Regehr WG, Tank WD (1991) Selective Fura-2 loading of presynaptic terminals and nerve cell processes by local perfusion in brain slice. *J Neurosci Methods* 37:111–119
- Ross WN, Salzberg BM, Cohen LB, Grinvald A, Davila HV, Waggoner AS, Wang CH (1977) Changes in absorption, fluorescence, dichroism, and birefringence in stained giant axons: optical measurement of membrane potential. *J Membrane Biol* 33:141–183
- Sinha SR, Patel S, Saggau P (1995) Simultaneous optical recording of evoked and spontaneous transients of membrane potential and intracellular calcium concentration with high spatio-temporal resolution. *J Neurosci Meth* 60:49–60
- Sinha SR, Saggau P (1996) Spontaneous synchronized activity in guinea pig hippocampal slices induced by 4-AP in the presence of ionotropic glutamate receptor antagonists. *Soc Neurosci Abstr* 22:823.17
- Sinha SR, Wu L-G, Saggau P (1997) Presynaptic calcium dynamics and transmitter release evoked by single action potentials at mammalian central synapses. *Biophys J* 72:637–651
- Tsien RY (1980) New calcium indicators and buffers with high selectivity against magnesium and protons: design, synthesis, and properties of prototype structures. *Biochemistry* 19:2396–2404
- Tsien RY (1981) A non-disruptive technique for loading calcium buffers and indicators into cells. *Nature* 290:527–528
- Wenner P, Tsau Y, Cohen LB, O'Donovan JH, Dan Y (1996) Voltage-sensitive dye recording using retrogradely transported dye in the chicken spinal cord: staining and signal characteristics. *J Neurosci Methods* 70:111–120
- Wu L-G, Saggau P (1994a) Presynaptic calcium is increased during normal synaptic transmission and paired-pulse facilitation, but not in long-term potentiation in area CA1 of hippocampus. *J Neurosci* 14:645–654

- Wu L-G, Saggau P (1994b) Pharmacological identification of two types of presynaptic voltage-dependent calcium channels at CA3-CA1 synapses of the hippocampus. *J Neurosci* 14:5613–5622
- Wu L-G, Saggau P (1994c) Adenosine inhibits evoked synaptic transmission primarily by reducing presynaptic calcium influx in area CA1 of hippocampus. *Neuron* 12:1139–1148
- Wu L-G, Saggau P (1995a) Block of multiple presynaptic channel types by  $\omega$ -conotoxin-MVIIC at hippocampal CA3 to CA1 synapses. *J Neurophysiol* 73:1965–1972
- Wu L-G, Saggau P (1995b) GABA<sub>B</sub> receptor-mediated presynaptic inhibition in guinea-pig hippocampus is caused by reduction of presynaptic Ca<sup>2+</sup> influx. *J Physiol (Lond)* 485:649–657
- Wu L-G, Saggau P (1997) Presynaptic inhibition of elicited neurotransmitter release. *TINS* 20:204–212
- Zecevic D (1996) Multiple spike-initiation zones in single neurons revealed by voltage-sensitive dyes. *Nature* 381:322–325

## ■ Suppliers

- Company: Molecular Probes, Eugene, OR, USA
- Company: Centronic, Newbury Park, CA, USA
- Company: Chroma Technology Corporation, Brattleboro, VT, USA
- Company: Fuji, Stamford, CT, USA
- Company: Hamamatsu, Bridgewater, NY, USA
- Company: Kepco, Flushing, NY, USA
- Company: Neuroplex, OptImaging, Fairfield, CT, USA
- Company: Vincent, Rochester, NY, USA
- Company: Zeiss, Rochester, NY, USA

## ■ Abbreviations

[Ca <sup>2+</sup> ] <sub>i</sub>	intracellular calcium concentration
CaSD	calcium-sensitive dye
CCD	charge-coupled device (camera)
DB	dichroic beamsplitter
EM	emission filter
EX	excitation filter
PDA	photodiode matrix amplifier
PDM	photodiode matrix
SH	shutter
V <sub>m</sub>	membrane potential
VSD	voltage-sensitive dye